Hyperfine Interact (2012) 209:111–115
DOI 10.1007/s10751-012-0565-z

Determination of the $D^*_{s0}(2317)$ width with the PANDA detector

Marius Christian Mertens for the PANDA collaboration

Published online: 24 January 2012

Abstract The $D^*_{s0}(2317)$ meson which was discovered at BaBar in 2003 has the interesting properties of a surprisingly narrow width and a mass just below the DK threshold. Different theoretical models try to explain the nature of its properties. A precise knowledge of the width is an important criterion to evaluate these models. However, only an upper limit of 3.8 MeV is known so far. A suitable method to determine the width of particles which are significantly narrower than the experimental mass resolution is to measure the production cross section as a function of the center of mass energy. The shape of this excitation function allows to deduce the width. At PANDA, the measurement of the production cross section will be possible in antiproton-proton collisions. The PANDA experiment at the future FAIR facility is designed to combine precisely adjustable beam momenta and high luminosities which make it an excellent tool for this kind of measurement. In the following we will describe the experimental procedure to carry out this measurement with the PANDA detector in order to achieve a resolution in the order of 0.1 MeV for the width of the $D^*_{s0}(2317)$.

Keywords PANDA · FAIR · $D^*_{s0}(2317)$ · Width · Excitation function

1 Introduction

Currently, various theoretical models exist which try to explain the nature of the $D^*_{s0}(2317)$ (e.g., [1, 2]). They feature different predictions for the width, making it an important experimental parameter to distinguish between the models. A direct width measurement by simply measuring the invariant mass distribution of the decay products only works where the experimental resolution is better than the width to

M. C. Mertens (✉)
Forschungszentrum Jülich GmbH, Wilhelm-Johnen-Strasse, 52428 Jülich, Germany
e-mail: m.mertens@fz-juelich.de

be measured. With a width less than 3.8 MeV [3], the $D_{s0}^{*}(2317)$ is too narrow for a direct width measurement. However, a resonance or threshold scan can be carried out instead which does not depend on the experimental mass resolution.

2 Experimental method

During an energy scan, the cross section is measured as a function of the center of mass energy. The shape of this excitation function depends on the particle width, thus the measurement of the shape can be used to deduce the particle width. With PANDA it is possible to study the reaction $\bar{p}p \rightarrow D_s^{\pm} D_{s0}^{*}(2317)^{\mp}$.

It has been shown in [4] (Section 4.2.4) that an inclusive reconstruction of the signal via $D_s^{\pm} \rightarrow \phi\pi^{\pm}, \quad \phi \rightarrow K^+K^-$ using the sum mass spectrum of the reconstructed D_s and the missing mass provides a promising combination of a relatively high signal count and good separation from the background which can be described by an Argus function. Therefore the following analysis is based on this reconstruction strategy.

Throughout the energy scan, the production rate of the $D_{s0}^{*}(2317)$ is measured for different beam momenta, i.e., center of mass energies. The experimental data then yield the mass and width of the $D_{s0}^{*}(2317)$ by fitting the excitation function ([4] Section 4.2.4, see (1)) to the scanpoints.

$$\frac{\sigma_{\Gamma}\left(\sqrt{s}\right)}{|M|^2} = \frac{\Gamma}{4\pi \cdot \sqrt{s}} \cdot \int_{-\infty}^{\sqrt{s}-m_{D_s}} \frac{\sqrt{\left(s-\left(m+m_{D_s}\right)^2\right) \cdot \left(s-\left(m-m_{D_s}\right)^2\right)}}{\left(m-m_{D_{s0}^{*}}\right)^2+\left(\frac{\Gamma}{2}\right)^2} dm \tag{1}$$

Note that (1) can be very well approximated by (2) below (Christoph Hanhart, priv. comm.). Here, m_{D_s} and $m_{D_{s0}^{*}}$ appear only as sum, which indicates that any deviation of m_{D_s} from the true D_s mass only causes a corresponding shift of the fitted $D_{s0}^{*}(2317)$ mass but has no influence on the reconstructed width.

$$\sigma(\lambda) \approx \sqrt{\left(m_{D_s}+m_{D_{s0}^{*}}\right) \cdot \Gamma} \cdot |M|^2 \cdot \frac{1}{2\pi} \cdot \int_{-\infty}^{\lambda} \frac{\sqrt{\lambda - x}}{x^2+1} dx \tag{2}$$

$$\lambda = \frac{2}{\Gamma} \cdot \left(\sqrt{s} - \left(m_{D_s}+m_{D_{s0}^{*}}\right)\right) \tag{3}$$

Beam momentum spread The individual antiprotons which form the beam follow a finite distribution around the nominal beam momentum, resulting in a finite distribution of the center of mass energy around the nominal value. The expected beam momentum spread of the HESR running in high luminosity mode is in the order of 10^{-4} [4] (Section 2.3.2.2) and results in a center of mass energy spread of 192 keV at the threshold energy (4286 MeV, 8802 MeV/c beam momentum). This effect is included in the simulations by convoluting the excitation function with a Gaussian bell curve which describes the momentum distribution of the antiproton beam.

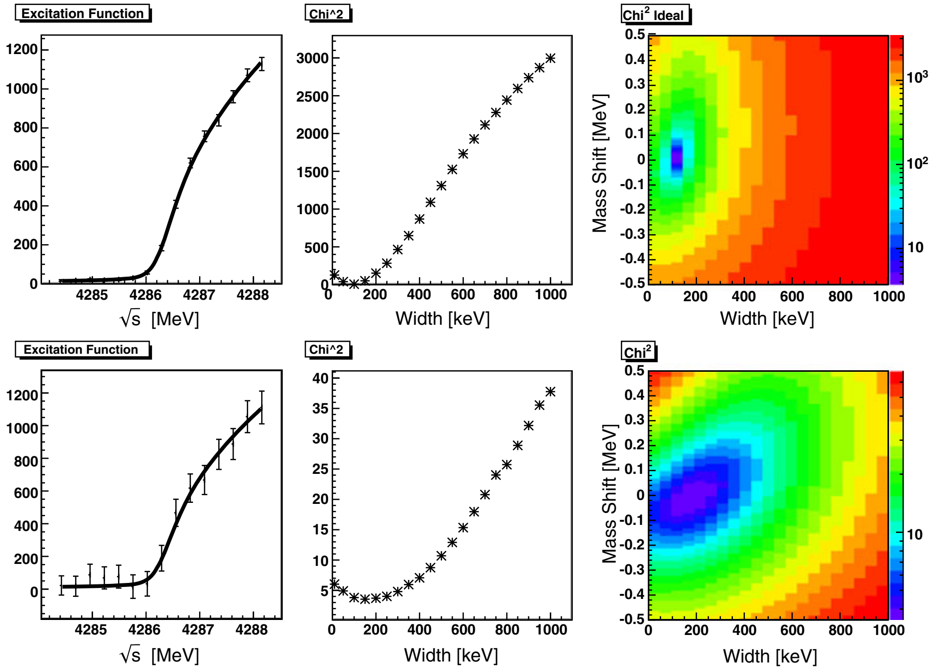

Fig. 1 Fit of the excitation function to simulated scan data for a 100 keV wide $D_{s0}^*(2317)$ and 60 days of total measurement time. The *upper row* shows the results without any background taken into account, the *lower row* includes an Argus background for a signal to background ratio of 1. *Left diagram:* simulated scan data drawn with an excitation function based on the input parameters. *Center:* χ^2 distribution for excitation functions with varying width hypotheses. *Right:* 2D χ^2 distribution for the excitation functions with varying mass and width hypotheses

3 Simulation overview

The following parameter space of the simulations is presented here: Relative beam momentum spread of 10^{-4}, 15 scanpoints in two energy ranges (± 1 MeV, ± 2 MeV) around the threshold, optionally two additional scanpoints located 4 MeV above the threshold, signal to background ratio of 1, 60 days total measurement time with a daily integrated luminosity of 9000 nb^{-1}, reconstruction efficiency of 0.25 (compare [4], Section 4.2.4).

While the specific background channels containing D_s mesons can be suppressed to half the signal size, the suppression of the generic background is more challenging. In [4] Section 4.2.4, a large suppression to $2 \cdot 10^{-5}$ has already been achieved, however there are still some parameters left for optimization (e.g. vertex and momentum constraints, pion identification). Since the optimization of kaon identification alone changed the background suppression by a factor of 10, an improvement of another order of magnitude to reach a total signal to background ratio of 1 seems feasible.

For historical reasons, the production cross section σ_0 has been normalized to the cross section of a 1 MeV wide $D_{s0}^*(2317)$ at threshold energy which corresponds to roughly 5 nb cross section 5 MeV above the threshold energy for $\sigma_0 = 1$.

Figure 1 shows the simulated signal counts for a 100 keV wide $D_{s0}^*(2317)$ together with a fit of the excitation function, where the parameters mass and width are found

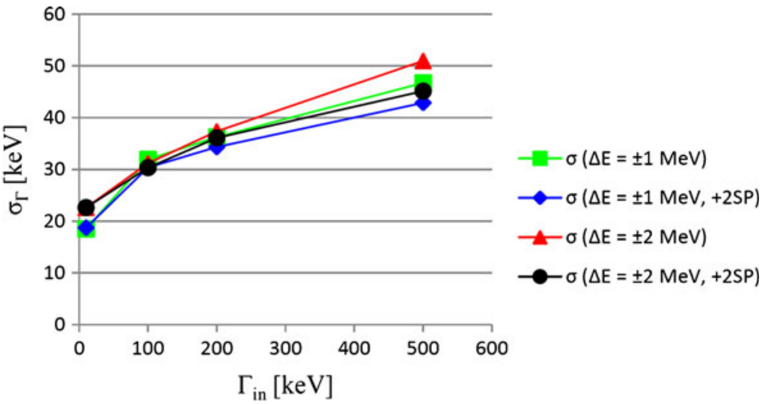

Fig. 2 Resulting resolutions for different $D^*_{s0}(2317)$ input widths. The four curves show the results for different scanpoint distributions around the threshold. The curves marked with +2SP feature two additional scanpoints located at 4 MeV above the threshold with otherwise identical scanpoint distributions

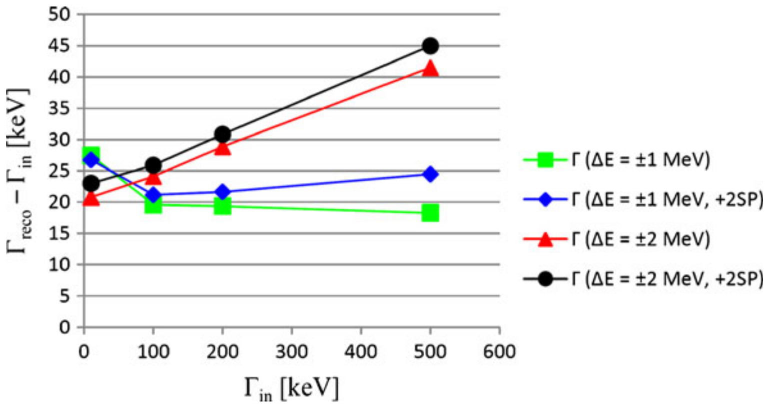

Fig. 3 Resulting deviations from the expectation value for different $D^*_{s0}(2317)$ input widths. The four curves show the results for different scanpoint distributions around the threshold. The curves marked with +2SP feature two additional scanpoints located at 4 MeV above the threshold with otherwise identical scanpoint distributions

by minimizing χ^2. The correlations which are observed when background is present might be related to the observation of an increased systematic deviation of the width from the expectation value with increasing background (compare Section 4). These correlations and in particular finding a strategy to eliminate their effect are subject to further study.

4 Results

Repeating the simulation and fitting procedures for different width hypotheses yields the expected resolutions (Fig. 2) and deviations from the expectation value (Fig. 3).

The statistical errors returned from the fit procedures were in all cases less than 3 keV (width resolution) and 6 keV (deviation from the expectation value). It becomes clear that the narrower energy range should be the location within which the final distribution of scanpoints should be optimized. The two additional scanpoints 4 MeV above the threshold do not improve the results but actually worsen it due to the increased background. The systematic deviations appear only with background, therefore it seems a reasonable assumption that this is a fit artifact which should be compensated in further studies. However, a conservative linear sum of the 50 keV resolution and 50 keV currently present systematic shift yields a very promising value of (100 ± 10) keV possible resolution.

For comparison: Leaving the other parameters unchanged, a resolution of 150 keV is obtained for a signal to background ratio of 0.1. The systematic deviation remains the same, indicating an overall resolution of (200 ± 10) keV for a 10 times larger background.

5 Conclusion

The resulting numbers for the systematic shift and the resolution indicate that a $D_{s0}^*(2317)$ width resolution in the order of 0.1 MeV is feasible. While for most experimental parameters the PANDA design values have been included into the simulations, the remaining main source of uncertainty is the as of yet unknown production cross section.

References

1. Faessler, A., et al.: Strong and radiative decays of the Ds(2317) meson in the DK-molecule picture. Phys. Rev. D **76**, 014005 (2007)
2. Guo, F.-K., et al.: More kaonic bound states and a comprehensive interpretation of the DsJ states. Phys. Rev. D **84**, 014013 (2011)
3. Nakamura, K., et al.: Particle data group. J. Phys. G **37**, 075021 (2010)
4. PANDA Collaboration: Physics Performance Report for PANDA. ArXiv:0903.3905v1[hep-ex] (2009)